Benefits of the Sentinel-2 mission triplet constellation in 2025

Katarzyna Ewa Lewińska [1,2], Olivier Hagolle [3], Ferran Gascon [4], Patrick Griffiths [5], Ulf Leser [6], Patrick Hostert [1,7]

[1] Geography Department, Humboldt-Universität zu Berlin, Unter den Linden 6, 10099 Berlin, Germany

[2] SILVIS Lab, Department of Forest and Wildlife Ecology, University of Wisconsin-Madison, 1630 Linden Drive, Madison WI 53706, USA

[3] CESBIO, Université de Toulouse, CNES/CNRS/INRAE/IRD/UT3, 18 avenue Edouard Belin BPI 2801, 31401 Toulouse Cedex 9, France

[4] European Space Agency (ESA), European Space Research Institute (ESRIN), Largo Galileo Galilei 1, Frascati, 00044, Italy

[5] European Space Agency (ESA), European Centre for Space Applications and Telecommunications (ECSAT), Harwell, OX11 0FD, United Kingdom

[6] Department of Computer Science, Humboldt-Universität zu Berlin, Unter den Linden 6, 10099 Berlin, Germany

[7] Integrative Research Institute on Transformations of Human-Environment Systems (IRI THESys), Humboldt-Universität zu Berlin, Unter den Linden 6, 10099 Berlin, Germany

*corresponding author: Katarzyna Ewa Lewińska

Abstract

With the first-year extension of Copernicus Sentinel-2A satellite operations nearing its end, an evaluation of its added-value is urgently needed. Here, we show that despite reduced spatio-temporal coverage, the additional Sentinel-2A acquisitions in 2025 enhanced the number of usable Sentinel-2 observations over Europe for the March-December period by almost 34%, and at the global scale by more than 21% for March-June. Furthermore, using regional and local examples, we demonstrate that the triplet Sentinel-2 constellation presents a clear advantage for land use and land cover change monitoring, as well as near-real-time observations, providing higher temporal fidelity and great potential for improved risk and disaster assessments, thus strengthening the capacity of research analyses and operational services alike. Overall, our results highlight the advantages of extending Sentinel-2A operational lifetime to maintain the triplet constellation of the Sentinel-2 mission.

Keywords

Copernicus, time series analysis, dense time series, data availability, usable data

1. Introduction

Thanks to the first-year extension of Sentinel-2A satellite operations, the Copernicus Sentinel-2 satellite mission has operated through most of 2025 with three active platforms (Copernicus, 2025). Sentinel-2A complements the Sentinel-2B and -2C baseline constellation since March 15, 2025 but operates with reduced spatial and temporal coverage, particularly outside of Europe and some other regions (Copernicus, 2026). Importantly, since its launch, Sentinel-2A showed no signs of deterioration in radiometric and spectral performance that may impact the quality of the data (S2 MSI ESL team, 2016). Since the current extension period approaches its end, it is timely and necessary to evaluate the added value of Sentinel-2A's extended operations as basis for the forthcoming decision on a potential further prolongation of its operational lifetime.

The Sentinel-2 mission supports research as well as a wide range of operational services and applications (Lefteris, Mamais et al., 2024). However, despite the mission's relatively high revisit time due to its original dual-platform setup, some applications are still challenged by the insufficient number of cloud-free observations at the pixel level related to regional differences in atmospheric conditions (Gao and Zhang, 2021; Main-Knorn et al., 2026; Watzig et al., 2023). Consequently, the experimental triplet constellation setup enhanced the Sentinel-2 mission operations in 2025 and created an opportunity to preview this configuration also in light of upcoming future missions such as Landsat Next (Portela et al., 2025) and Sentinel-2 NG.

Although the absolute number of additional Sentinel-2 acquisitions enabled by the triplet constellation could serve as a basic measure of the success of the mission's extended operation (Figure S1), these metrics alone do not capture the practical added value of the data in terms of effective (cloud free, pixel level) observations. To demonstrate the

qualitative improvements arising from the Sentinel-2A mission extension and how they enhance downstream applications we:

- evaluate the amount of cloud-, snow-, and shade-free data (hereafter *usable observations*) acquired by each Sentinel-2 satellite between March through June 2025 (global extent) and March through December 2025 (European extent);
- evaluate the difference in quality of standard national vegetation monitoring products derived using acquisitions from all three Sentinel-2 satellites and the Sentinel-2B and -2C baseline;
- highlight specific examples when Sentinel-2A observations significantly enhanced terrestrial mapping and monitoring.

2. Methods

2.1. Sentinel-2 data availability

For data availability analysis and the examples of Sentinel-2A acquisitions enhancing terrestrial mapping and monitoring, we used the Sentinel-2 top-of-atmosphere (TOA) reflectance Level-1C scenes acquired between 1 January 2025 and 31 December 2025, which we accessed through Google Earth Engine (Gorelick et al., 2017) between September 2025 and January 2026. To identify cloud- snow-, and shade-free acquisitions we employed the methodology implemented by Lewińska et al. (2023, 2024), which relies on the inherent QA60 cloud mask and B10 bands (Aybar et al., 2022; Main-Knorn et al., 2017), Cloud Probability product (Skakun et al., 2022), Cloud Displacement Analysis (Frantz et al., 2018), snow mask branch of the Sen2Cor processor (Main-Knorn et al., 2017), and object-based identification of cloud shadows based on scene-specific sun parameters. For more conservative results we further employed a 40-m buffer around each identified cloud and cloud-shadow object.

To create the global overview of usable Sentinel-2 data, we sampled individual pixels spacing them 0.18° apart in the latitudinal and longitudinal directions as defined in the WGS 84 (EPSG:4326) projection. This resulted in 475,150 sample points located over land between -179.8867°W and 179.5733°E and 83.50834°N and -59.05167°S. To demonstrate the added value of Sentinel-2A acquisitions, we compared the data record comprising usable Sentinel-2A observations with the baseline comprising acquisitions made by Sentinel -2B and -2C. Due to the computational demands of the above workflow and the need for timeliness, the spatial coverage of the March-December analysis was limited to Europe.

To further inspect data availability for equidistant cloud-free temporal composites required by certain applications, we simulated the 5-, 10-day and monthly composites by recording the number of available observations for each aggregation period and classified a composite as "successful" if at least one valid observation was present. We set 1 January as the starting date of the compositing window sequence. If the final compositing window was shorter than half of its defined width, it was merged with the preceding composite. We calculated the percentage increase in data availability enabled by Sentinel-2A acquisitions as the proportion between the unique Sentinel-2A acquisitions or composites and the corresponding number of data or composites provided by the Sentinel-2B and -2C baseline constellation. Since we were interested only in unique Sentinel-2 pixel-level acquisitions, we excluded Sentinel-2 pixel-level observations that for any given day were already depicted by Sentinel-2B or -2C. When there was no data or composites in the Sentinel-2B and -2C baseline, the final proportion of the increase was defined by the number of additional datasets or composites derived from Sentinel-2A multiplied by 100%, i.e., one unique Sentinel-2A acquisition counts as a 100% increase over the no-data baseline.

For the March-June 2025 global analysis we stratified the results at the continental and regional levels based on the ESRI's dataset of World Continents (Esri). For the

Europe-specific analyses, we based our statistics of the March-December 2025 acquisitions on biogeographical regions (Roekaerts, 2002) to better capture the regional variability. Importantly, the spatial extend of this Europe-specific dataset excludes Atlantic islands and extends eastwards only to 66.9° N, 47.26° E - 46.04° N, 49.14° E transect, i.e., excluding the most eastern region of the European part of Russia.

2.2. Monthly composites

To provide a real-life example of Sentinel-2-based national-scale products used for land cover classification and agricultural monitoring we derived monthly November composites for France and Germany. We selected November due to challenging meteorological conditions and the importance of this period for winter- and cover-crop monitoring (Lobert et al., 2025). For France, we followed the standard processing of the THEIA land data center using the Weighted Average Synthesis Processor (WASP), which for each pixel computes a weighted average of all valid observations (cloud, shade and snow-free) during a synthesis period of 45 days centered on the 15th of the respective month, here the 15th of November. The weights favor observations acquired far from clouds, with a low aerosol content, and closer to the 15th of the month (Hagolle et al., 2018). When all the cloud-free observations are snow covered, the average of snow reflectance is provided. For permanently cloud-covered pixels, the average of cloud reflectance is provided. The quality of the syntheses benefits from the Multi-Mission Atmospheric Correction and Cloud Screening (MACCS) - Atmospheric and Topographic Correction (ATCOR) Joint Algorithm (MAJA) cloud masking and atmospheric correction processor, characterized by a very low rate of cloud omissions (Baetens et al., 2019; Colin et al., 2023; Skakun et al., 2022).

For Germany, we derived the November monthly average composites based on the Level 2 top-of-atmosphere (TOA) data processed following the standard ARD processing of FORCE (Framework for Operational Radiometric Correction for Environmental monitoring

processing engine; Frantz, 2019) We downloaded all Sentinel-2 scenes with cloud cover below 70% from the Copernicus Open Access Hub. We next processed them including atmospheric and topographic corrections, adjusted for reflectance from pixel adjacency and directional reflectance effects (Buchner et al., 2020; Frantz et al., 2016; Roy et al., 2017), and performed cloud and cloud-shadow masking (Frantz et al., 2018; Zhu et al., 2015; Zhu and Woodcock, 2012). Furthermore, we co-registered each Sentinel-2 scene to the pre-existing Landsat mosaic (Rufin et al., 2021; Yan et al., 2018). Such data processing standard is used by multiple research groups and institutions in Germany and worldwide, and constitutes a subset of the German-wide ARD data cube reproduced on the CODE-DE that offers data and cloud processing for German authorities (CODE-DE). To derive the monthly November 2025 composites for Sentinel-2B and -2C, and Sentinel-2A, -2B, and -2C constellations, we used the Time Series Analysis module of FORCE to calculate the average value for the respective time window using the previously processed Sentinel-2 Level 2 data.

3. Results

3.1. Data availability

Our results indicate that at the global scale, between March and June 2025, the triplet Sentinel-2 constellation captured up to 58 (mean 12.8, median 11, SD=9.75; Table A.1) per-pixel usable observations (Figure 1c). Sentinel-2A alone contributed up to 15 (mean 2.24, median 2, SD=2.28; Figure 1a) unique observations, i.e., observations with no spatio-temporal overlap with acquisitions provided by the Sentinel-2B and -2C baseline (mean 10.55, median 9, SD=8.21; Figure 1b), which translated into a global mean per-pixel proportional increase of over 21% in the data availability (median 16.67%, SD=27,84%; Figure 1d, Table A.2). Notably, the Mediterranean basin and the tropical regions in Africa received the greatest number of unique usable Sentinel-2A observations, which closely reflects the configuration of the extended mission (Copernicus, 2026). When inspected at the

continental scale, the contribution of Sentinel-2A for March through June was the greatest in Africa, where on average, 4.68 additional pixel-level useful observations were recorded (median 4, SD=2.38, mean increase of 37.07%; Table A.1 and Table A.2). Australia also benefited substantially, with an average of 3.22 new acquisitions (median 3, SD=1.4, mean increase of 20.65%). In Europe, Sentinel-2A added on average 2.64 usable acquisitions (median 2, SD=2.01, mean increase of 29.02%), followed closely by South America, with a mean of 2.44 unique acquisitions (median 2, SD=1.95, mean increase of 41,45%). The added value of Sentinel-2A acquisitions in Asia, North America and Oceania was more modest (Table A.1 and Table A.2).

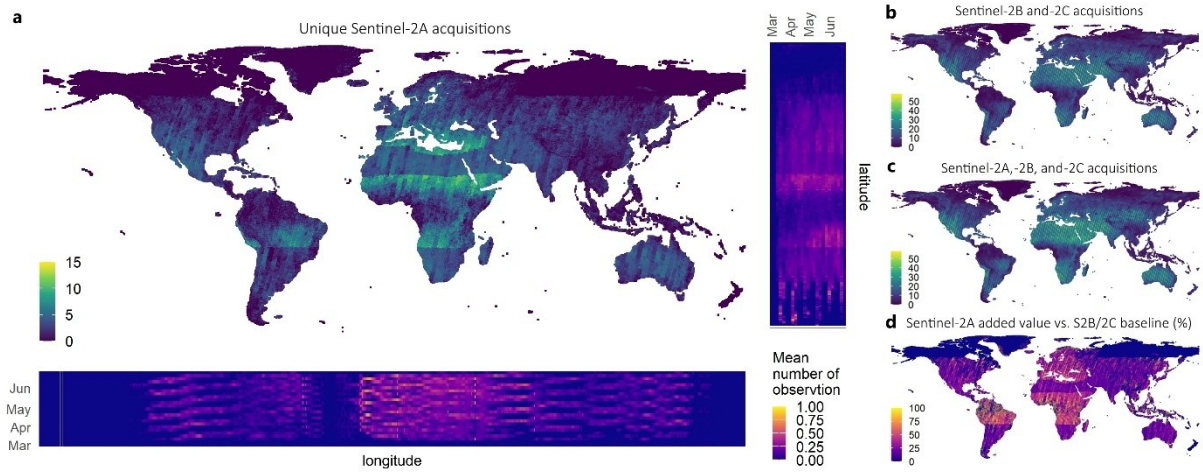

Figure 1 Unique cloud- snow-, and shade-free pixel-level acquisitions made by Sentinel-2A from March through June 2025 (a). Side plots in (a) depict the latitude- and longitude-specific five-day means of usable acquisitions made by Sentinel-2A for the corresponding period. Side panels depict: (b) all usable acquisitions made by Sentinel-2B and -2C during the March-June period, (c) all usable acquisitions made by all three Sentinel-2 platforms during the March-June period, and (d) relative increase (%) in the number of usable acquisitions enabled by Sentinel-2A as compared to the Sentinel-2B and -2C baseline for the March-June period. All visualizations in WGS 84 projection. Full-size versions of panels b-d in Figures S2-4. Global and continent-specific statistics on the number of acquisitions in Table A.1 and proportional changes between triplet and dual constellation configurations in Table A.2.

When comparing availability of March-June observations within 5- and, 10-day, and monthly synthetic composites derived based on the triplet and dual Sentinel-2 constellations (Table A.1), not surprisingly, the 5-day composites showed the greatest pixel-level increase in observation frequency when including Sentinel-2A (Figure S7 and S9, Table A.1). The triplet constellation provided between March and June 2025, on average, 1.57 additional

5-day composites in Africa (median 1, SD=1.32, mean increase of 18.15%; Table A.1 and A.2), 1.31 in Europe (median 1, SD=1.24, mean increase of 18.89%), and 1.29 in South America (median 1, SD=1.17, mean increase of 29.84%). The added value of Sentinel-2A acquisitions in the triplet constellation on 10-day and monthly composites was comparatively modest, with the greatest gains in South America (Table A.1 and A.2).

In Europe (spatially defined as in Figure 2), the benefits arising from the Sentinel-2 triplet constellation were distinct for March through December 2025. All three Sentinel-2 satellites together captured up to 113 per-pixel usable observations (mean 34.06, SD=19.75; Figure 2a,Table A.3), with Sentinel-2A contributing up to 28 unique observations (mean 8.23, SD=4.93, mean increase of 33.92%; Figure 2b,Table A.4). The south of Europe received the greatest number of unique Sentinel-2A observations, with on average over 15 new observations in the Anatolian, Mediterranean, and over 12 in Black Sea and Pannonian biogeographical regions (Table A.3). Importantly, the overall increase in the number of observations enabled by Sentinel-2A ranged between 23.61% (Arctic) and 44.90% (Pannonian; Table A.4), and indicated apparent gains across the continent (Figure 2d).

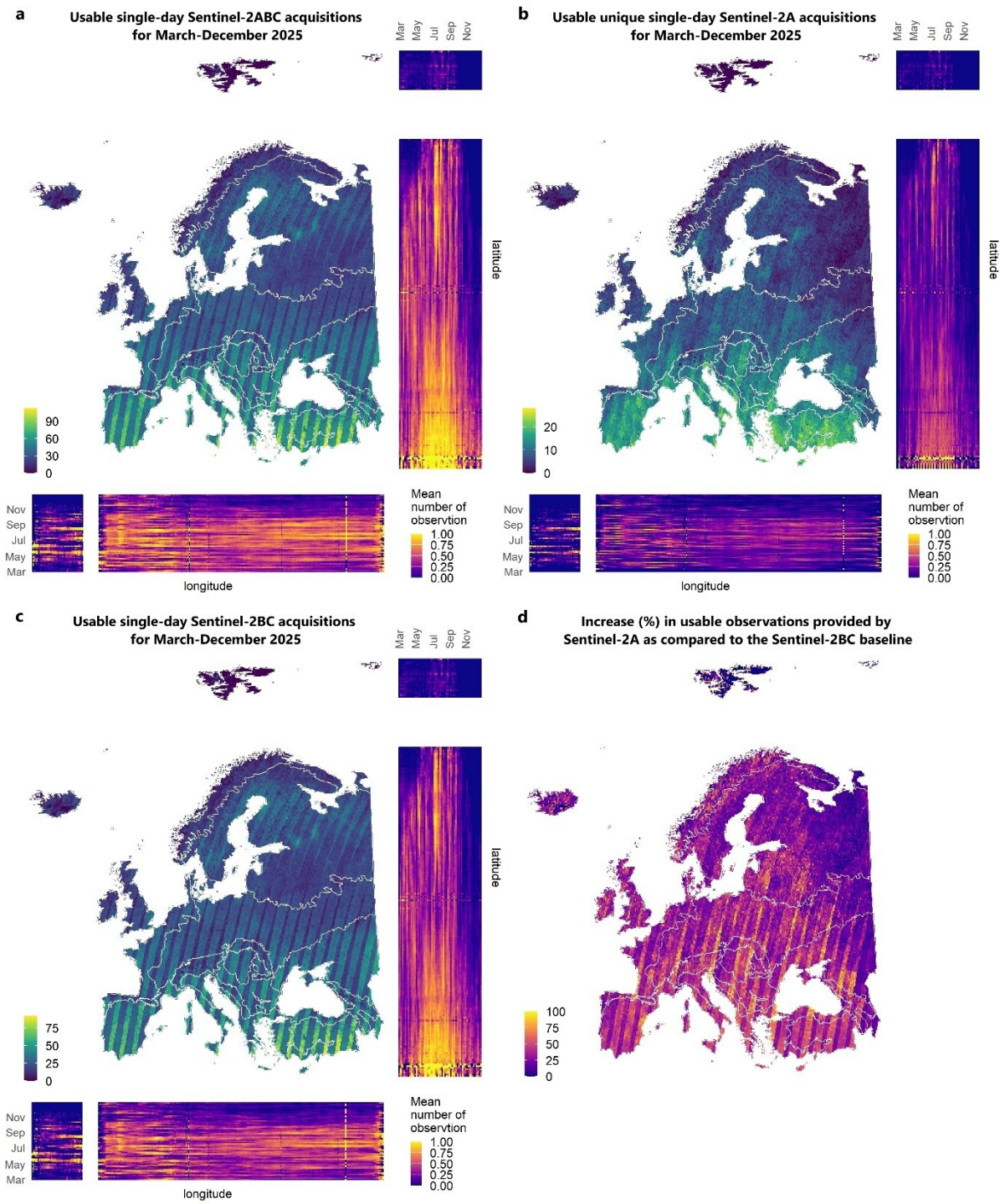

Figure 2 Comparison of the number of single-day usable (i.e., cloud- snow-, and shade-free) observations acquired from March through December 2025 by (a) Sentinel-2A, -2B, and -2C, and (c) Sentinel-2B and -2C. In (b) unique single-day March-December 2025 acquisitions enabled by Sentinel-2A and in (d) the proportional increase (in %) enabled by unique single-day Sentinel-2A acquisitions as compared with the Sentinel-2B and -2C baseline. Side panels show the latitude- and longitude-specific means of usable acquisitions made by the corresponding combination of platforms, aggregated to 5-day composites for better visual readability. Biogeographical regions are marked with white lines and defined in Figure S10. All panels plotted in WGS 84 projection.

This March-December Sentinel-2 data pool over Europe allowed to derive up to 59 5-day composites, out of which up to 16 new composites were enabled by the Sentinel-2A

acquisitions (Figure S12). The greatest increase in data coverage at pixel-level occurred in the southern regions, where, on average, five new 5-day composites were added across the observation period (Table A.3). However, the greatest proportional increase of new composites occurred where the orbits do not overlap (Table S12d).

3.2. Monthly composites

The real-life example of Sentinel-2-based national-scale monthly composites clearly shows the superiority of the triplet constellation expressed in fewer missing and cloud-contaminated pixels. For France (Figure 5), incorporating Sentinel-2A acquisitions into the 45-day synthetic images reduced the cloud presence, especially in the western and central parts of the country. We noted even greater advantages for monthly November composites derived for Germany (Figure 4). When including Sentinel-2A acquisitions into the 30-day target window, we were able to greatly reduce the share of missing and clouded pixels, though the wall-to-wall coverage was still not achievable.

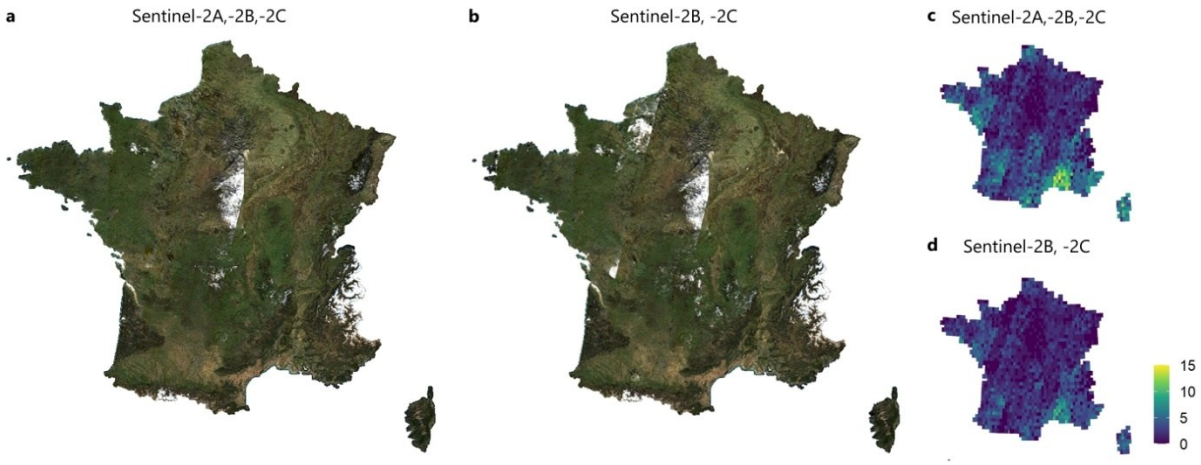

Figure 3 Monthly weighted average syntheses for entire France based on 45 days centered on the 15th day of each month, here for November 2025. In (a) composite based on all three Sentinel-2 satellites and in (b) from only Sentinel-2B and -2C. The clouds are present in both composites, with a significantly lower image quality when only Sentinel-2B and -2C were used. The overview of usable acquisitions for the corresponding time and sensor combinations in (c) and (d) respectively. All panels in Lambert_93 projection.

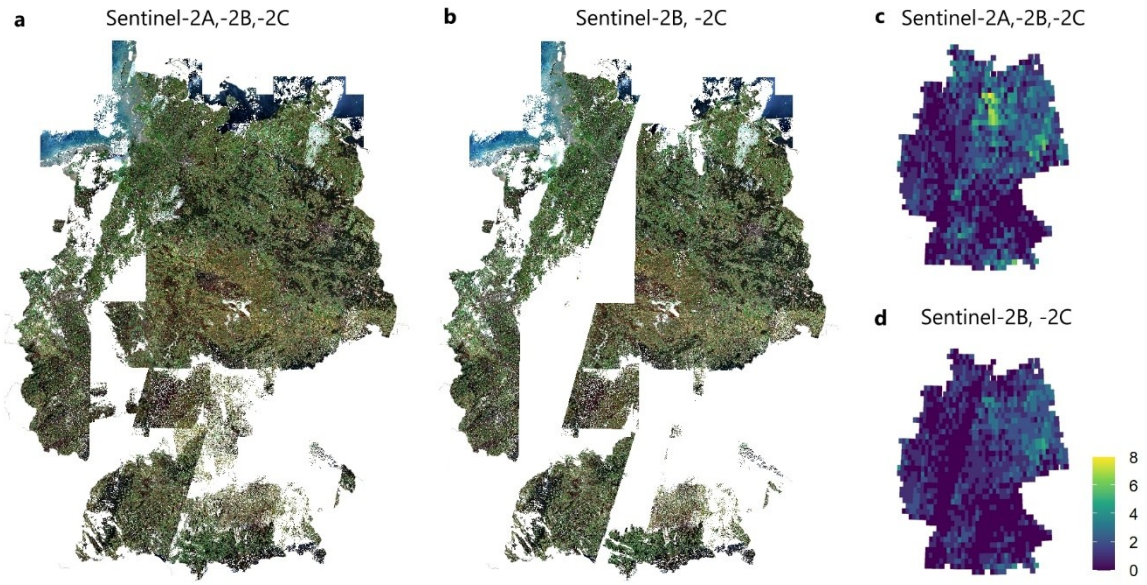

Figure 4 Monthly average composite (RGB) for November 2025, based on top-of-atmosphere (TOA) data processed following the standard Analysis Ready Data (ARD) processing of FORCE. In (a) composite based on all three Sentinel-2 satellites and in (b) from only Sentinel-2B and -2C. The clouds are present in both composites, with a significantly lower image quality when only Sentinel-2B and -2C were used. The overview of usable acquisitions for the corresponding time and sensor combinations are shown in (c) and (d), respectively. All panels plotted in ETRS89-LAEA projection.

3.3. Specific examples

Beyond statistics, the added-value of additional Sentinel-2A observations depends on the land surface and its dynamics, and the respective downstream application. For example, high data density facilitates characterization of crop phenology and stress conditions during critical growth stages (Figure 5a) (Main-Knorn et al., 2026). In managed grasslands, dense time series reinforce the detection of mowing events or grazing (Figure 5b), thereby providing a better understanding of grassland productivity and the intensity of management practices (Reinermann et al., 2022; Schwieder et al., 2022). In monitoring natural vegetation, dense time series allow for more confident land cover/vegetation type attribution (Figure 5c) (Blickensdörfer et al., 2022) and, among others, more precise quantification of ecosystem carbon dynamics (Besnard et al., 2025). Furthermore, dense time series enable the timely attribution and detection of disturbance events, such as deforestation (Figure 5d) and degradation (Figure 5e), where capturing the explicit timing of

an event is essential to establish liability and to implement optimized post-disturbance management (Pickens et al., 2025).

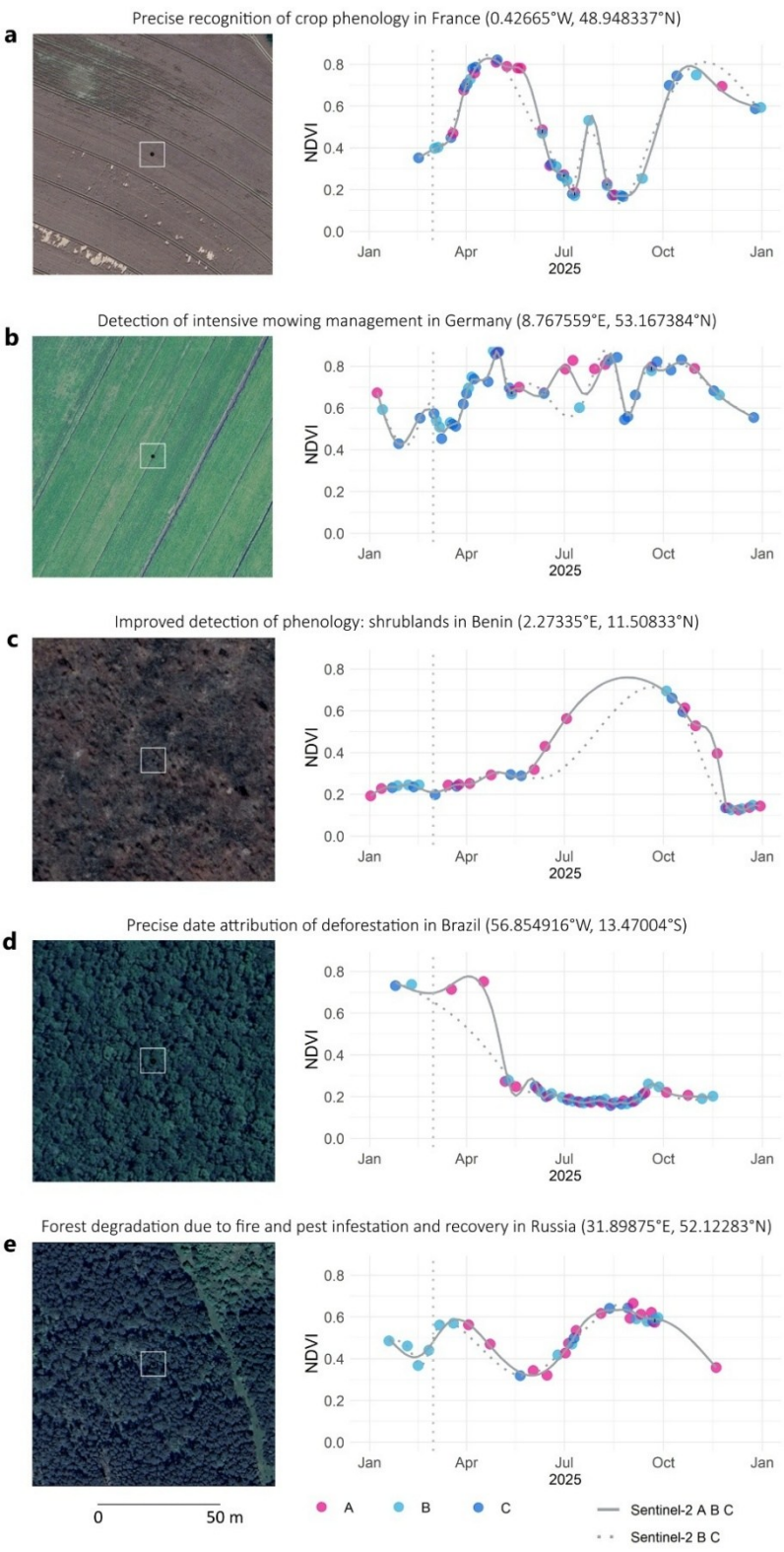

Figure 5 Five examples of the added value of Sentinel-2A observations, as compared with the Sentinel-2B and -2C baseline, for different land cover/land use classes depicted with corresponding NDVI time series. Each VHR insert (image sourced: Google Earth, accessed in early January 2026) represents 100x100m centered at the sampled pixel (10x10m; gray bounding box). Attribution of NDVI value to a specific Sentinel-2 platform is done with color. NDVI drops in b (July) and d (April) were verified by inspecting the respective Sentinel-2 scenes to exclude cloud contamination. NDVI curves were fitted using natural splines. Vertical dotted line marks March 1, allowing to evaluate the triplet acquisitions starting from March 15.

4. Discussion

The distribution of usable Sentinel-2 observations was highly heterogeneous in time and space, reflecting the overall mission design and the meteorological conditions. The Sentinel-2A data pool was further defined by the strategic acquisition plan, which primarily focused on Europe and tropical regions (Copernicus, 2026). This created continental but also regional and local variations in the Sentinel-2A data availability, and thus shaped the added value of the extension. Notably, in Europe substantial relative increase in data availability enabled by Sentinel-2A acquisitions occurred outside the orbit overlaps i.e., where the temporal fidelity is systematically lower.

Despite a considerable increase in data availability enabled by the Sentinel-2A acquisitions, achieving full off-season monthly coverage for France and Germany remained challenging, particularly under stricter compositing criteria. Nevertheless, the additional acquisitions improve the quality of monitoring and reporting for many EU policies, including those focused on agriculture and sustainability (Berger et al., 2026, 2025). Data scarcity, however, is still an issue especially in regions and during time periods with high cloud-cover probability. Importantly, higher data density increases the likelihood of 'well-timed' acquisitions, which are most critical for many applications (Main-Knorn et al., 2026).

Owing to the significant variability in meteorological conditions and land use/land cover types, coupled with the wide range of mapping and monitoring approaches, determining the exact added value of Sentinel-2A within the triplet Sentinel-2 constellation remains challenging. While our analysis shows clear potential benefits and quantifies the availability of usable observations, further studies are required to assess the specific gains for distinct regions and downstream applications.

5. Conclusions

Overall, our analysis illustrates the added value of the extended Sentinel-2A operation in 2025. Despite its reduced acquisition scenario, Sentinel-2A enhanced the quality of a diverse range of potential downstream applications in need of near-real-time and retrospective analyses aimed at monitoring and managing of terrestrial ecosystems. Therefore, the results also highlight the potential of a triplet constellation to increase the value and capacity of operational services, such as those provided by the Copernicus program. The benefits of the Sentinel-2 triplet constellation were apparent across many geographies, with high relevance of the additional observations especially in regions with systematically lower temporal fidelity in the Sentinel-2B and -2C baseline, specifically including areas outside the orbit overlaps. In general, the experimental Sentinel-2 triplet constellation demonstrated its added value for Copernicus products and services that benefit from the higher temporal observation frequency, thereby backing EU's climate and sustainability goals. As such, our results clearly demonstrate the benefits of extending the Sentinel-2A mission's lifetime and indicate the general potential of a triplet constellation setup.

Data availability

Data and codes supporting the analysis are available at 10.5281/zenodo.18803215. Furthermore, availability of usable Copernicus Sentinel-2A, -2B, and -2C January-July 2025 acquisitions can be interactively queried using the dedicated Google Earth Engine (GEE) app: https://katarzynaelewinska.users.earthengine.app/view/sentinel-2abc-2025. Due to the need for timeliness given the satellite mission design, we here present global time series for March-June 2025, while extended processing for entire 2025 is ongoing and will be added to the GEE data app once being finalized.

Acknowledgements

The research presented in this paper was funded by the Deutsche Forschungsgemeinschaft (DFG, German Research Foundation) – Project-ID 414984028 – SFB 1404 FONDA.

Contributions

Katarzyna Ewa Lewińska: conceptualization, data curation, formal analysis, investigation, methodology, visualization, writing – original draft, writing – review and editing;

Olivier Hagolle: data curation, formal analysis, visualization, writing – original draft, writing – review and editing; Ferran Gascon: visualization, writing – review and editing; Patrick Griffiths: writing – review and editing; Ulf Leser: funding acquisition, project administration, writing – review and editing; Patrick Hostert: conceptualization, funding acquisition, supervision, writing – review and editing.

Appendix A

Table A.1 Mean number of daily acquisitions by the respective Sentinel-2 platforms between March and June 2025, with median and standard deviation (SD) values, alongside corresponding statistics for 5-, 10-day and monthly composites. The numbers are aggregated at the global and continental scales, and show: (a) unique observations and composites enabled by Sentinel-2A, (b) combined observations by Sentinel-2A, -2B, and -2C, and (c) by Sentinel-2B and -2C only. Definition of adopted boundaries of continents according to Figure S5.

Region	1 day			5-day			10-day			monthly		
	mean	median	SD	mean	median	SD	mean	median	SD	mean	median	SD
Unique Sentinel-2A acquisitions												
Global	2.24	2	2.28	0.88	1	1.10	0.47	0	0.77	0.08	0	0.30
Africa	4.68	4	2.38	1.57	1	1.32	0.75	0	0.95	0.10	0	0.34
Asia	1.68	1	1.93	0.62	0	0.86	0.31	0	0.58	0.06	0	0.24
Australia	3.22	3	1.40	0.88	1	0.91	0.35	0	0.61	0.03	0	0.19
Oceania	0.16	0	0.60	0.11	0	0.42	0.09	0	0.36	0.04	0	0.21
South America	2.44	2	1.95	1.29	1	1.17	0.86	1	0.93	0.26	0	0.51
Europe	2.64	2	2.01	1.31	1	1.24	0.76	0	0.92	0.11	0	0.33
North America	1.00	0	1.51	0.46	0	0.82	0.25	0	0.56	0.04	0	0.21
Combined Sentinel-2A, -2B, and -2C acquisitions												
Global	12.80	11	9.75	10.05	10	6.68	6.93	7	3.92	3.01	4	1.31
Africa	19.98	20	9.69	15.38	17	5.64	9.90	11	2.66	3.83	4	0.52
Asia	12.44	10	9.65	9.78	9	6.51	6.72	7	3.72	2.96	3	1.22
Australia	20.55	20	8.45	16.11	17	4.49	10.25	11	2.11	3.92	4	0.35
Oceania	7.02	6	4.88	6.46	6	4.08	5.40	5	2.93	3.00	3	1.12
South America	10.52	9	7.36	8.80	8	5.32	6.63	7	3.28	3.23	4	1.01
Europe	12.62	12	6.80	9.71	10	4.62	7.23	8	3.08	3.37	4	1.09
North America	8.09	6	8.27	6.41	5	6.03	4.67	4	4.00	2.16	2	1.57
Combines Sentinel-2B and -2C acquisitions												
Global	10.55	9	8.21	9.17	8	6.39	6.47	7	3.84	2.93	4	1.33
Africa	15.30	15	8.45	13.82	15	5.93	9.15	10	3.02	3.72	4	0.68
Asia	10.76	9	8.28	9.15	8	6.26	6.41	6	3.66	2.90	3	1.23
Australia	17.33	16	7.77	15.23	16	4.68	9.90	11	2.27	3.89	4	0.42
Oceania	6.86	6	4.88	6.35	6	4.10	5.31	5	2.94	2.96	3	1.14
South America	8.08	7	6.27	7.50	7	5.17	5.77	6	3.33	2.97	3	1.14
Europe	9.98	10	5.54	8.40	9	4.23	6.47	7	2.93	3.26	4	1.13
North America	7.09	5	7.17	5.95	5	5.66	4.40	4	3.82	2.12	2	1.55

Table A.2 Summary statistics (mean, median, standard deviation (SD), min, and max) of proportional increase in availability of cloud-, snow-, and shade-free acquisitions provided by the triple Sentinel-2 constellation between March and June 2025, as compared to the Sentinel-2B, and -2C baseline for the same period. Next to the single-day acquisitions, statistics for 5-, 10-day, and monthly composites are provided. Definition of adopted boundaries of continents according to Figure S5.

Region	1 day					5-day					10-day					monthly				
	mean	median	SD	min	max	mean	median	SD	min	max	mean	median	SD	min	max	mean	median	SD	min	max
Global	21.65	16.67	27.84	0	700	12.68	4.76	25.04	0	700	10.03	0.00	24.41	0	600	4.56	0.00	19.54	0	400
Africa	37.07	31.25	26.88	0	500	18.15	10.53	26.82	0	500	13.64	0.00	26.58	0	500	5.27	0.00	20.74	0	400
Asia	14.75	11.11	19.96	0	500	8.33	0.00	17.64	0	500	6.37	0.00	17.33	0	500	2.91	0.00	14.91	0	300
Australia	20.65	20.00	12.61	0	400	7.64	5.56	12.24	0	400	4.85	0.00	12.12	0	400	1.48	0.00	10.10	0	300
Oceania	4.27	0.00	17.81	0	200	3.47	0.00	16.45	0	200	3.26	0.00	16.08	0	200	2.40	0.00	14.45	0	200
South America	41.45	30.00	46.23	0	700	29.84	16.67	45.39	0	700	26.38	12.5	45.07	0	600	15.67	0.00	37.55	0	400
Europe	29.02	25.00	28.61	0	500	18.89	12.5	26.13	0	500	14.75	9.09	25.08	0	500	5.34	0.00	19.04	0	400
North America	10.40	0.00	18.58	0	500	6.73	0.00	16.40	0	500	5.27	0.00	15.74	0	500	2.12	0.00	12.35	0	300

Table A.3 Mean number of daily acquisitions, 5-, 10-day and monthly, composited enabled by Sentinel-2A acquisitions between March and December 2025 for biogeographical regions of Europe with corresponding median and standard deviation (SD) values. Definition of adopted boundaries of biogeographical regions according to Figure S10. The area considered for the statistics is smaller than the European continent outlined in Figure S5 and corresponds to the footprint depicted in Figure 2.

Region	1 day			5-day			10-day			monthly		
	mean	median	SD	mean	median	SD	mean	median	SD	mean	median	SD
Unique Sentinel-2A acquisitions												
Overall	8.23	7	4.93	3.66	3	2.38	2.03	2	1.61	0.36	0	0.62
Alpine	7.30	7	4.38	3.54	3	2.38	2.07	2	1.68	0.42	0	0.66
Anatolian	17.56	18	3.17	4.91	4	2.89	1.65	1	1.54	0.13	0	0.36
Arctic	2.10	2	2.05	1.17	1	1.32	0.83	1	1.04	0.29	0	0.55
Atlantic	7.42	7	2.86	3.90	4	2.02	2.54	2	1.58	0.54	0	0.75
Black Sea	12.49	13	3.36	5.96	6	2.74	2.74	2	2.01	0.51	0	0.66
Boreal	5.43	5	2.71	2.79	3	1.91	1.65	1	1.38	0.28	0	0.54
Continental	8.40	8	3.61	4.16	4	2.19	2.41	2	1.68	0.45	0	0.68
Mediterranean	15.78	16	3.72	5.22	5	2.65	2.35	2	1.66	0.26	0	0.50
Pannonian	12.62	13	3.84	5.07	5	2.20	2.61	2	1.81	0.25	0	0.51
Steppic	8.71	8	3.52	3.72	3	2.21	1.96	2	1.51	0.37	0	0.62
Combined Sentinel-2A, -2B, and -2C acquisitions												
Overall	34.06	31	16.75	24.99	24	10.11	17.85	18	5.77	8.09	8	1.87
Alpine	27.83	24	15.07	20.67	19	10.36	15.28	15	6.67	7.22	7	2.44
Anatolian	64.36	8	19.79	43.04	43	6.73	26.11	27	2.84	9.67	10	0.69
Arctic	12.15	12	9.88	8.81	9	6.85	6.85	7	5.11	3.83	4	2.57
Atlantic	30.19	29	11.00	22.96	23	7.28	17.34	18	4.52	8.58	9	1.46
Black Sea	45.37	41	15.09	33.86	34	6.74	23.33	23	3.23	9.53	10	0.81
Boreal	27.88	27	8.56	20.68	21	5.29	15.55	16	3.45	7.44	8	1.18
Continental	33.10	32	11.86	25.23	25	7.14	18.55	19	4.03	8.58	9	1.16
Mediterranean	56.38	51	18.06	38.95	39	7.34	24.75	25	3.12	9.80	10	0.53
Pannonian	43.56	46	12.10	31.41	32	5.72	22.11	22	2.74	9.53	10	0.65
Steppic	39.11	28	13.07	28.78	29	7.10	20.19	20	3.84	8.68	9	1.04
Combines Sentinel-2B and -2C acquisitions												
Overall	25.84	24	13.14	21.33	20	9.41	15.82	16	5.65	7.73	8	1.94
Alpine	20.53	18	11.75	17.16	15	9.45	13.20	12	6.24	6.80	7	2.45
Anatolian	46.8	39	18.34	38.13	38	8.09	24.45	25	3.41	9.54	10	0.78
Arctic	10.02	10	8.47	7.63	7	6.20	6.02	6	4.67	3.54	4	2.48
Atlantic	22.77	21	9.29	19.06	19	6.81	14.80	15	4.49	8.04	8	1.65
Black Sea	32.88	29	13.49	27.90	27	7.87	20.59	21	4.12	9.02	9	1.04
Boreal	22.45	21	7.45	17.98	18	4.99	13.89	14	3.39	7.15	7	1.25
Continental	24.69	24	9.57	21.07	21	6.84	16.14	16	4.21	8.12	8	1.35
Mediterranean	40.59	35	15.92	33.73	33	8.01	22.40	23	3.66	9.55	10	0.75
Pannonian	30.94	33	10.20	26.35	27	6.64	19.50	20	3.62	9.28	9	0.87
Steppic	30.40	30	12.00	25.06	25	7.66	18.22	18	4.41	8.31	8	1.24

Table A.4 Summary statistics (mean, median, standard deviation (SD), min, and max) of proportional increase in availability of cloud-, snow-, and shade-free acquisitions provided by the triple Sentinel-2 constellation between March and June 2025, as compared to the Sentinel-2B, and -2C baseline for the same period. Next to the single-day acquisitions, statistics for 5-, 10-day, and monthly composites are provided. Definition of adopted boundaries of biogeographical regions according to Figure S10. The area considered for the statistics is smaller than the European continent outlined in Figure S5 and corresponds to the footprint depicted in Figure 2.

Region	1 day					5-day					10-day					monthly				
	mean	median	SD	min	max	mean	median	SD	min	max	mean	median	SD	min	max	mean	median	SD	min	max
Overall	33.92	30.77	19.64	0	400	19.80	16.47	16.92	0	350	15.14	11.11	16.22	0	350	5.91	0	12.69	0	300
Alpine	38.49	35.00	21.81	0	233.33	24.13	20.00	20.08	0	200	18.94	14.29	19.70	0	200	8.35	0	17.00	0	200
Anatolian	42.01	43.42	13.76	0	88.89	14.58	11.76	10.69	0	77.78	7.45	4.35	7.65	0	46.67	1.56	0	4.41	0	42.86
Arctic	23.61	15.38	33.47	0	400	18.89	8.33	31.47	0	300	16.87	6.25	30.23	0	300	11.22	0	28.14	0	300
Atlantic	36.08	32.43	17.23	0	200	23.13	20.00	15.82	0	200	19.81	15.89	16.48	0	160	8.30	0	13.68	0	150
Black Sea	43.28	39.62	18.45	0	114.29	25.08	20.69	17.14	0	92.86	15.35	10.53	13.73	0	64.29	6.37	0	8.64	0	50
Boreal	26.11	23.53	15.15	0	266.67	17.13	14.28	14.18	0	266.67	13.26	10.00	13.20	0	266.67	4.71	0	9.98	0	150
Continental	37.25	33.33	19.12	0	350	22.53	19.05	16.95	0	350	17.42	13.33	17.18	0	350	6.70	0	11.72	0	200
Mediterranean	43.04	41.67	14.60	0	108.33	17.32	14.71	11.65	0	93.33	11.50	9.09	9.45	0	70	3.06	0	6.27	0	75
Pannonian	44.90	41.56	18.73	10.87	114.29	22.42	17.86	15.75	0	100	15.39	11.88	13.80	0	81.82	3.13	0	6.65	0	40
Steppic	33.47	28.57	19.63	2.27	200	18.01	13.33	15.75	0	160	12.98	9.52	13.54	0	140	5.41	0	10.27	0	133.33

References

Aybar, C., Ysuhuaylas, L., Loja, J., Gonzales, K., Herrera, F., Bautista, L., Yali, R., Flores, A., Diaz, L., Cuenca, N., Espinoza, W., Prudencio, F., Llactayo, V., Montero, D., Sudmanns, M., Tiede, D., Mateo-García, G., Gómez-Chova, L., 2022. CloudSEN12, a global dataset for semantic understanding of cloud and cloud shadow in Sentinel-2. Sci. Data 9, 782. https://doi.org/10.1038/s41597-022-01878-2

Baetens, L., Desjardins, C., Hagolle, O., 2019. Validation of Copernicus Sentinel-2 Cloud Masks Obtained from MAJA, Sen2Cor, and FMask Processors Using Reference Cloud Masks Generated with a Supervised Active Learning Procedure. Remote Sens. 11, 433. https://doi.org/10.3390/rs11040433

Berger, K., Foerster, S., Szantoi, Z., Hostert, P., Foerster, M., Van De Kerchove, R., Vancutsem, C., Schweitzer, C., Masolele, R., Reiche, J., Dowell, M., Enssle, F., Suarez, D.R., Nepomshina, O., Herold, M., 2025. Evolving Earth observation capabilities for recent land-related EU policies. Land Use Policy 158, 107749. https://doi.org/10.1016/j.landusepol.2025.107749

Berger, K., Hostert, P., Schlerf, M., Immitzer, M., Szantoi, Z., Okujeni, A., Foerster, S., Colditz, R., Giardino, C., Machwitz, M., Weiss, M., Defourny, P., Kutser, T., Remeta, P., Foerster, M., Féret, J.-B., Asadzadeh, S., Chabrillat, S., Croft, H., Stassin, T., Schickling, A., Vancutsem, C., Celesti, M., Proud, S., Jonckheere, I., Strobl, P., Milewski, R., Herold, M., 2026. Advancing optical earth observation for EU policies: needs, opportunities, recommendations. Environ. Sci. Eur. 38, 52. https://doi.org/10.1186/s12302-026-01346-3

Besnard, S., Viana-Soto, A., Hartmann, H., Patacca, M., Heinrich, V.H.A., Kowalski, K., Santoro, M., De Keersmaecker, W., Van De Kerchove, R., Herold, M., Senf, C., 2025. Natural disturbances increasingly affect Europe's most mature and carbon-rich forests. https://doi.org/10.5194/egusphere-2025-6288

Blickensdörfer, L., Schwieder, M., Pflugmacher, D., Nendel, C., Erasmi, S., Hostert, P., 2022. Mapping of crop types and crop sequences with combined time series of Sentinel-1, Sentinel-2 and Landsat 8 data for Germany. Remote Sens. Environ. 269, 112831. https://doi.org/10.1016/j.rse.2021.112831

Buchner, J., Yin, H., Frantz, D., Kuemmerle, T., Askerov, E., Bakuradze, T., Bleyhl, B., Elizbarashvili, N., Komarova, A., Lewińska, K.E., Rizayeva, A., Sayadyan, H., Tan, B., Tepanosyan, G., Zazanashvili, N., Radeloff, V.C., 2020. Land-cover change in the Caucasus Mountains since 1987 based on the topographic correction of multi-temporal Landsat composites. Remote Sens. Environ. 248, 111967. https://doi.org/10.1016/j.rse.2020.111967

CODE-DE - About [WWW Document], n.d. URL https://code-de.org/en/about/ (accessed 2.25.26).

Colin, J., Hagolle, O., Landier, L., Coustance, S., Kettig, P., Meygret, A., Osman, J., Vermote, E., 2023. Assessment of the Performance of the Atmospheric Correction Algorithm MAJA for Sentinel-2 Surface Reflectance Estimates. Remote Sens. 15, 2665. https://doi.org/10.3390/rs15102665

Copernicus, 2026. Sentinel-2 Acquisition Plans - Sentinel Online [WWW Document]. Sentin. Online. URL https://sentinels.copernicus.eu/copernicus/sentinel-2/acquisition-plans (accessed 1.6.26).

Copernicus, 2025. OBSERVER: Sentinel-2A extending operations to meet user needs | Copernicus [WWW Document]. URL https://www.copernicus.eu/en/news/news/observer-sentinel-2a-extending-operations-meet-user-needs?utm_source=chatgpt.com (accessed 1.6.26).

Esri, Global Mapping International (GMI), n.d. World Continents [WWW Document]. URL https://hub.arcgis.com/datasets/esri::world-continents/ (accessed 2.9.26).
Frantz, D., 2019. FORCE—Landsat + Sentinel-2 Analysis Ready Data and Beyond. Remote Sens. 11, 1124. https://doi.org/10.3390/rs11091124
Frantz, D., Haß, E., Uhl, A., Stoffels, J., Hill, J., 2018. Improvement of the Fmask algorithm for Sentinel-2 images: Separating clouds from bright surfaces based on parallax effects. Remote Sens. Environ. 215, 471–481. https://doi.org/10.1016/j.rse.2018.04.046
Frantz, D., Roder, A., Stellmes, M., Hill, J., 2016. An Operational Radiometric Landsat Preprocessing Framework for Large-Area Time Series Applications. IEEE Trans. Geosci. Remote Sens. 54, 3928–3943. https://doi.org/10.1109/TGRS.2016.2530856
Gao, F., Zhang, X., 2021. Mapping Crop Phenology in Near Real-Time Using Satellite Remote Sensing: Challenges and Opportunities. J. Remote Sens. 2021, 2021/8379391. https://doi.org/10.34133/2021/8379391
Gorelick, N., Hancher, M., Dixon, M., Ilyushchenko, S., Thau, D., Moore, R., 2017. Google Earth Engine: Planetary-scale geospatial analysis for everyone. Remote Sens. Environ. 202, 18–27. https://doi.org/10.1016/j.rse.2017.06.031
Hagolle, O., Morin, D., Kadiri, M., 2018. Detailed Processing Model For The Weighted Average Synthesis Processor (Wasp) For Sentinel-2. https://doi.org/10.5281/ZENODO.1401359
Lefteris, Mamais, Geoff, Sawyer, Daire, Boyle, Julia, Caufape, 2024. Sentinel Benefits Study Demonstrating the value of Sentinel Data through Rigorous Value Chain Analyses and Powerful User Stories.
Lewińska, K., Frantz, D., Leser, U., Hostert, P., 2023. Usable Observations over Europe: Evaluation of Compositing Windows for Landsat and Sentinel-2 Time Series. https://doi.org/10.20944/preprints202308.2174.v2
Lewińska, K.E., Ernst, S., Frantz, D., Leser, U., Hostert, P., 2024. Global overview of usable Landsat and Sentinel-2 data for 1982–2023. Data Brief 111054. https://doi.org/10.1016/j.dib.2024.111054
Lobert, F., Schwieder, M., Alsleben, J., Broeg, T., Kowalski, K., Okujeni, A., Hostert, P., Erasmi, S., 2025. Unveiling year-round cropland cover by soil-specific spectral unmixing of Landsat and Sentinel-2 time series. Remote Sens. Environ. 318, 114594. https://doi.org/10.1016/j.rse.2024.114594
Main-Knorn, M., Nendel, C., Flores, L., Krugmann, C., Inforsato, L., Ghazaryan, G., 2026. Evaluating the impact of PlanetScope and Sentinel-2 data fusion on maize phenometrics retrieval. GIScience Remote Sens. 63, 2637207. https://doi.org/10.1080/15481603.2026.2637207
Main-Knorn, M., Pflug, B., Louis, J., Debaecker, V., Müller-Wilm, U., Gascon, F., 2017. Sen2Cor for Sentinel-2, in: Bruzzone, L., Bovolo, F., Benediktsson, J.A. (Eds.), Image and Signal Processing for Remote Sensing XXIII. Presented at the Image and Signal Processing for Remote Sensing, SPIE, Warsaw, Poland, p. 3. https://doi.org/10.1117/12.2278218
Pickens, A.H., Hansen, M.C., Song, Z., Poulson, A., Komarova, A., Baggett, A., Kerr, T., Mikus, A., Ortiz Dominguez, C., Tyukavina, A., Lima, A., 2025. Rapid monitoring of global land change. Nat. Commun. 16, 8948. https://doi.org/10.1038/s41467-025-64014-9
Portela, B., Van Der Werff, H., Hecker, C., Van Der Meijde, M., 2025. Landsat Next current design for geological remote sensing: VNIR-SWIR-TIR data continuity and new opportunities. Sci. Remote Sens. 12, 100258. https://doi.org/10.1016/j.srs.2025.100258

Reinermann, S., Gessner, U., Asam, S., Ullmann, T., Schucknecht, A., Kuenzer, C., 2022. Detection of Grassland Mowing Events for Germany by Combining Sentinel-1 and Sentinel-2 Time Series. Remote Sens. 14, 1647. https://doi.org/10.3390/rs14071647

Roekaerts, M., 2002. The Biogeographical Regions Map of Europe Basic principles of its creation and overview of its development.

Roy, D., Li, Z., Zhang, H., 2017. Adjustment of Sentinel-2 Multi-Spectral Instrument (MSI) Red-Edge Band Reflectance to Nadir BRDF Adjusted Reflectance (NBAR) and Quantification of Red-Edge Band BRDF Effects. Remote Sens. 9, 1325. https://doi.org/10.3390/rs9121325

Rufin, P., Frantz, D., Yan, L., Hostert, P., 2021. Operational Coregistration of the Sentinel-2A/B Image Archive Using Multitemporal Landsat Spectral Averages. IEEE Geosci. Remote Sens. Lett. 18, 712–716. https://doi.org/10.1109/LGRS.2020.2982245

S2 MSI ESL team, 2016. Data Quality Report Sentinel-2 L1C MSI January 2026 (No. OMPC.CS.DQR.01.12-2025).

Schwieder, M., Wesemeyer, M., Frantz, D., Pfoch, K., Erasmi, S., Pickert, J., Nendel, C., Hostert, P., 2022. Mapping grassland mowing events across Germany based on combined Sentinel-2 and Landsat 8 time series. Remote Sens. Environ. 269, 112795. https://doi.org/10.1016/j.rse.2021.112795

Skakun, S., Wevers, J., Brockmann, C., Doxani, G., Aleksandrov, M., Batič, M., Frantz, D., Gascon, F., Gómez-Chova, L., Hagolle, O., López-Puigdollers, D., Louis, J., Lubej, M., Mateo-García, G., Osman, J., Peressutti, D., Pflug, B., Puc, J., Richter, R., Roger, J.-C., Scaramuzza, P., Vermote, E., Vesel, N., Zupanc, A., Žust, L., 2022. Cloud Mask Intercomparison eXercise (CMIX): An evaluation of cloud masking algorithms for Landsat 8 and Sentinel-2. Remote Sens. Environ. 274, 112990. https://doi.org/10.1016/j.rse.2022.112990

Watzig, C., Schaumberger, A., Klingler, A., Dujakovic, A., Atzberger, C., Vuolo, F., 2023. Grassland cut detection based on Sentinel-2 time series to respond to the environmental and technical challenges of the Austrian fodder production for livestock feeding. Remote Sens. Environ. 292, 113577. https://doi.org/10.1016/j.rse.2023.113577

Yan, L., Roy, D.P., Li, Z., Zhang, H.K., Huang, H., 2018. Sentinel-2A multi-temporal misregistration characterization and an orbit-based sub-pixel registration methodology. Remote Sens. Environ. 215, 495–506. https://doi.org/10.1016/j.rse.2018.04.021

Zhu, Z., Wang, S., Woodcock, C.E., 2015. Improvement and expansion of the Fmask algorithm: cloud, cloud shadow, and snow detection for Landsats 4–7, 8, and Sentinel 2 images. Remote Sens. Environ. 159, 269–277. https://doi.org/10.1016/j.rse.2014.12.014

Zhu, Z., Woodcock, C.E., 2012. Object-based cloud and cloud shadow detection in Landsat imagery. Remote Sens. Environ. 118, 83–94. https://doi.org/10.1016/j.rse.2011.10.028

Benefits of the Sentinel-2 mission triplet constellation in 2025

Supplement

Katarzyna Ewa Lewińska [1,2], Olivier Hagolle [3], Ferran Gascon [4], Patrick Griffiths [5], Ulf Leser [6], Patrick Hostert [1,7]

[1] Geography Department, Humboldt-Universität zu Berlin, Unter den Linden 6, 10099 Berlin, Germany

[2] SILVIS Lab, Department of Forest and Wildlife Ecology, University of Wisconsin-Madison, 1630 Linden Drive, Madison WI 53706, USA

[3] CESBIO, Université de Toulouse, CNES/CNRS/INRAE/IRD/UT3, 18 avenue Edouard Belin BPI 2801, 31401 Toulouse Cedex 9, France

[4] European Space Agency (ESA), European Space Research Institute (ESRIN), Largo Galileo Galilei 1, Frascati, 00044, Italy

[5] European Space Agency (ESA), European Centre for Space Applications and Telecommunications (ECSAT), Harwell, OX11 0FD, United Kingdom

[6] Department of Computer Science, Humboldt-Universität zu Berlin, Unter den Linden 6, 10099 Berlin, Germany

[7] Integrative Research Institute on Transformations of Human-Environment Systems (IRI THESys), Humboldt-Universität zu Berlin, Unter den Linden 6, 10099 Berlin, Germany

*corresponding author: Katarzyna Ewa Lewińska
lewinska@hu-berlin.de
phone +49 (0)30 2093-45823

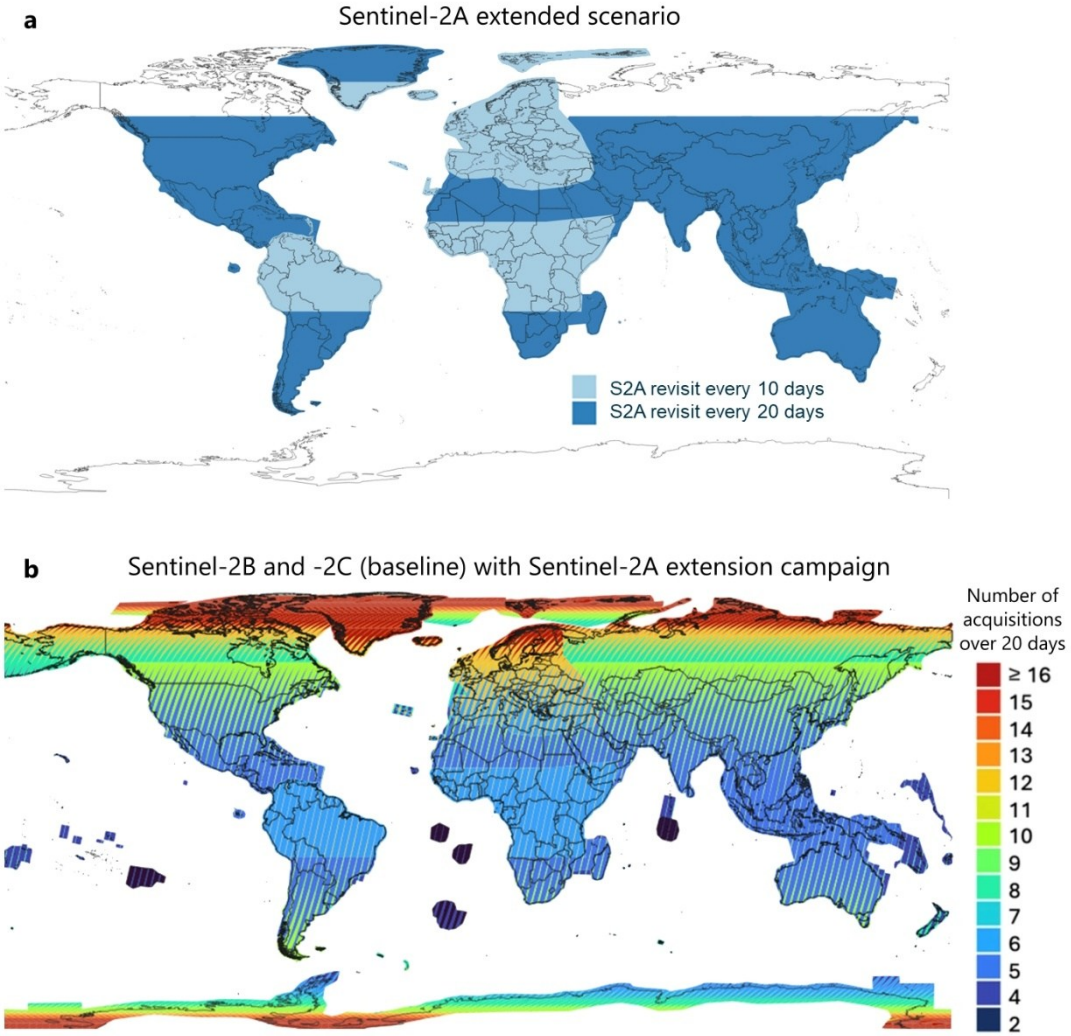

Figure S1 Sentinel-2 mission acquisition plans for (a) Sentinel-2A extended scenario and (b) the overall number of acquisitions made over a 20-day period accounting for Sentinel-2B and -2C (baseline – dual constellation) with Sentinel-2A extension campaign.

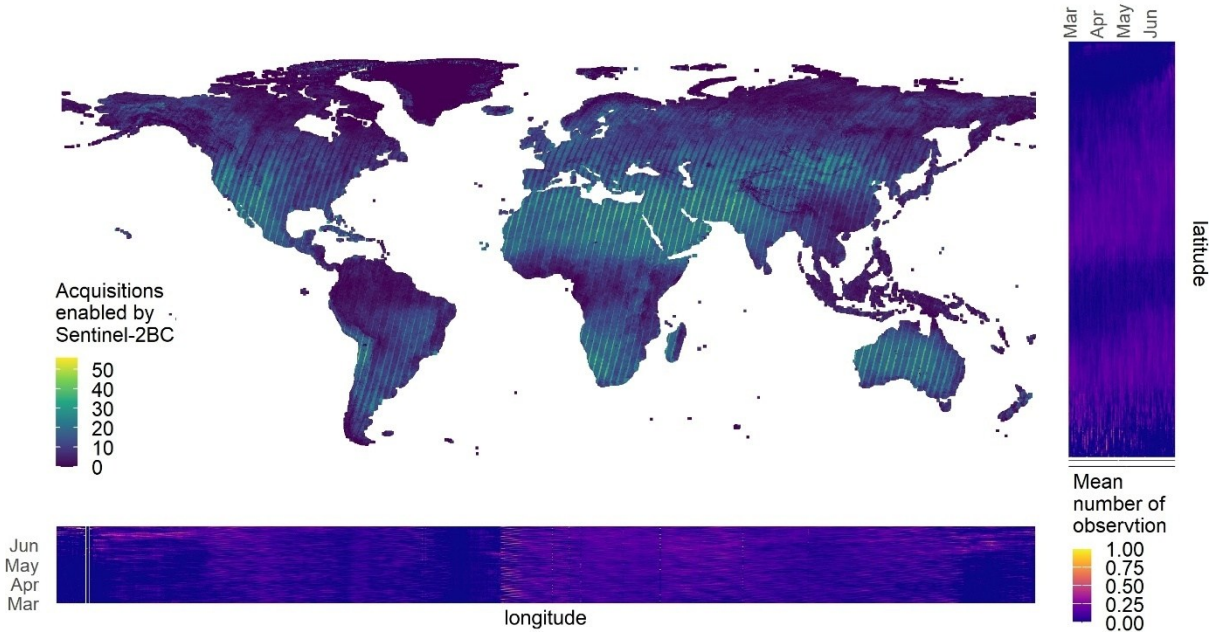

Figure S2 Cloud- snow-, and shade-free pixel-level acquisitions made by Sentinel-2B and -2C from March through June 2025. Side plots depict the latitude- and longitude-specific mean number of usable acquisitions made each day. Figure is in WGS 84 projection.

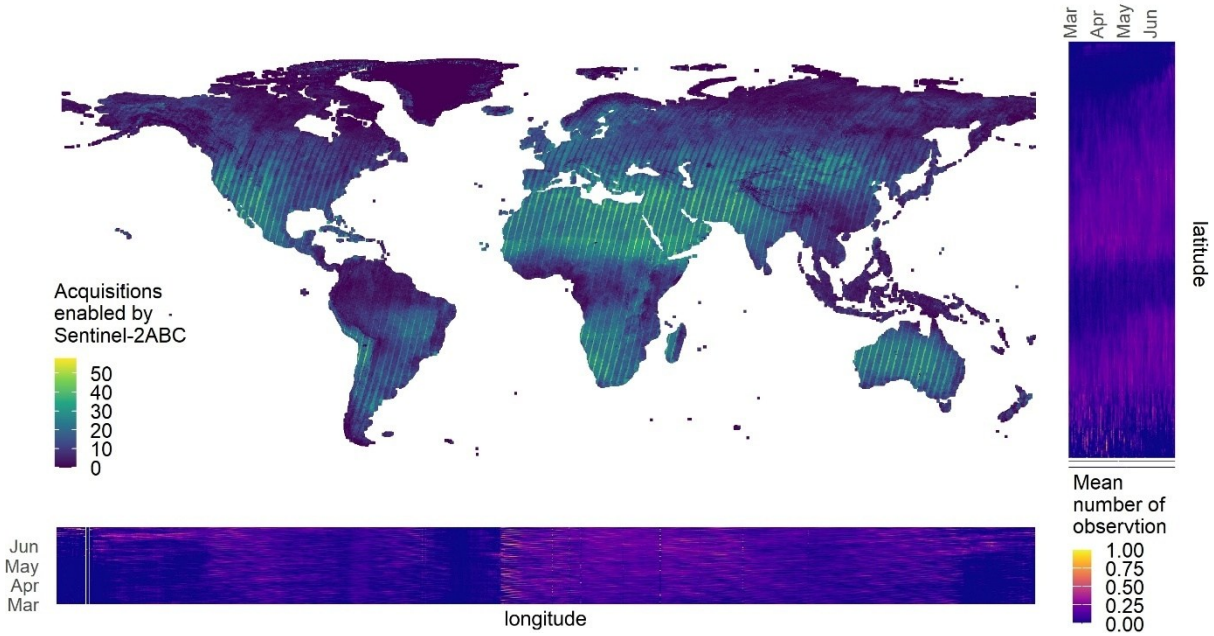

Figure S3 Cloud- snow-, and shade-free pixel-level acquisitions by Sentinel-2A, -2B, and -2C from March through June 2025. Side plots depict the latitude- and longitude-specific mean number of usable acquisitions made each day. Figure is in WGS 84 projection.

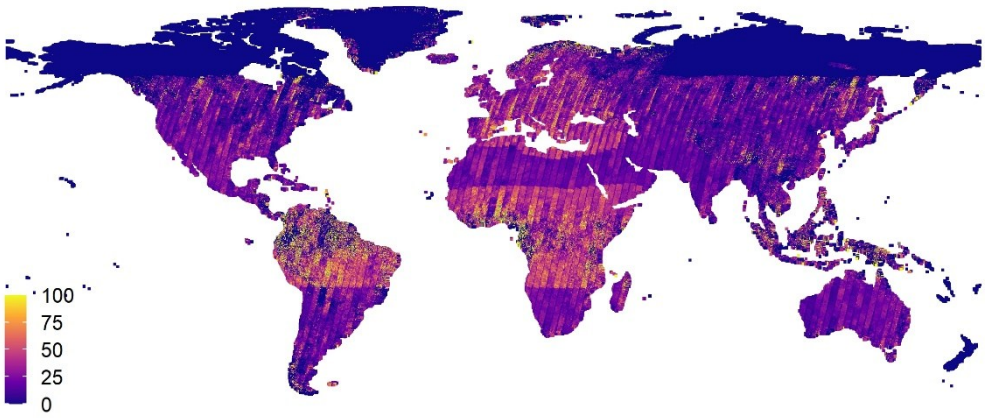

Figure S4 Proportional increase (%) in the number of cloud- snow-, and shade-free pixel-level Sentinel-2A acquisitions from March through June 2025 as compared to the Sentinel-2B, and -2C baseline data pool. Figure is in WGS 84 projection.

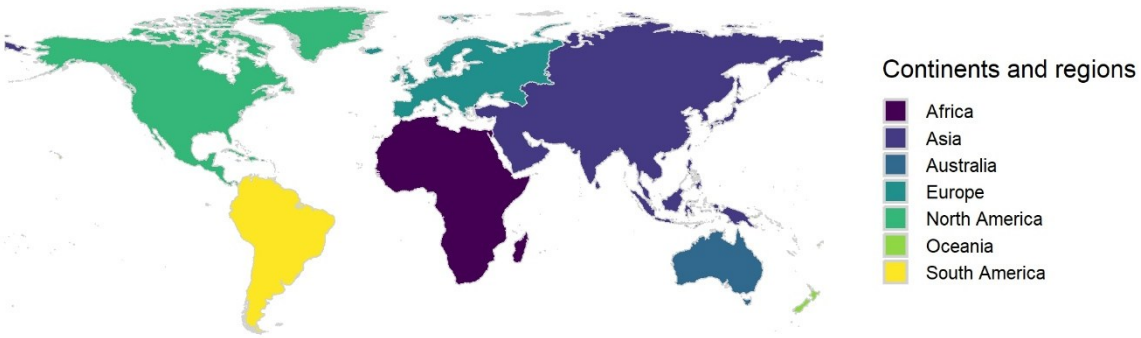

Figure S5 Boundaries of the continents and regions adopted in this study. Source: Esri, Global Mapping International (GMI). Figure is in WGS 84 projection.

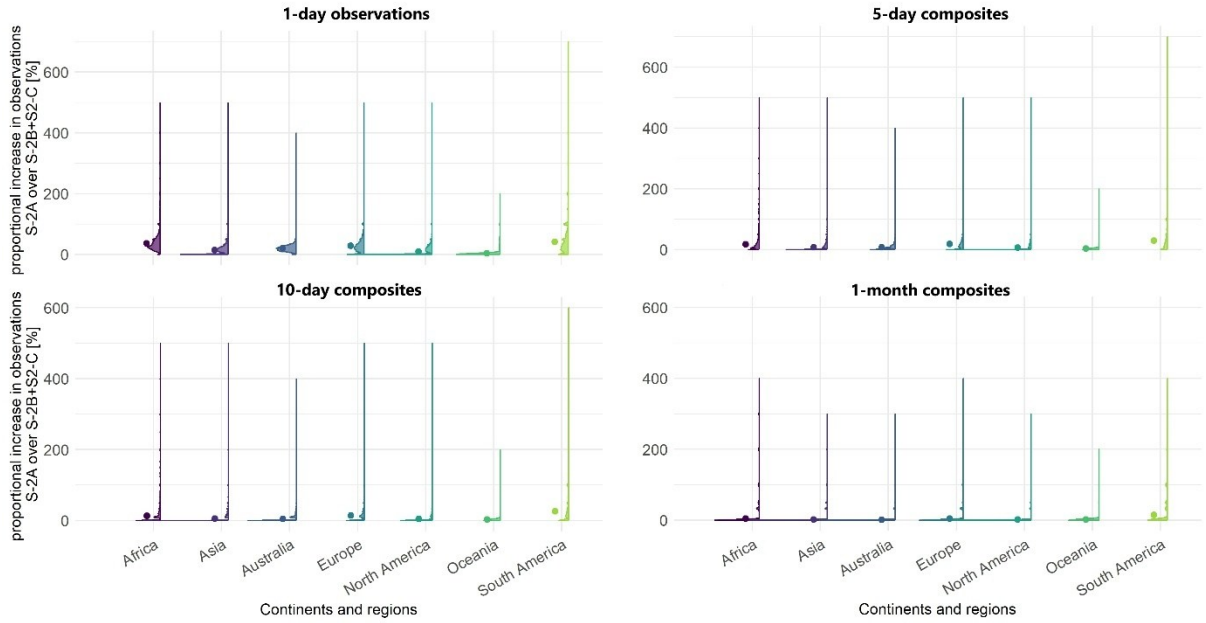

Figure S6 Violin plots showing distribution of the proportional increase (in %) ensured by Sentinel-2A usable observations and multi-day composites as compared to the Sentinel-2B and -2C baseline across continents and main regions. The mean value for each distribution is represented by a dot. The width of each plot illustrates the relative number of observations in each bin. When no usable acquisitions were provided by the Sentinel-2B and -2C baseline, the number of acquisitions added by Sentinel-2A was multiplied by 100%, i.e., values >100% include areas without any useful acquisitions by Sentinel-2B and -2C. Definition of adopted boundaries of continents according to Figure S5.

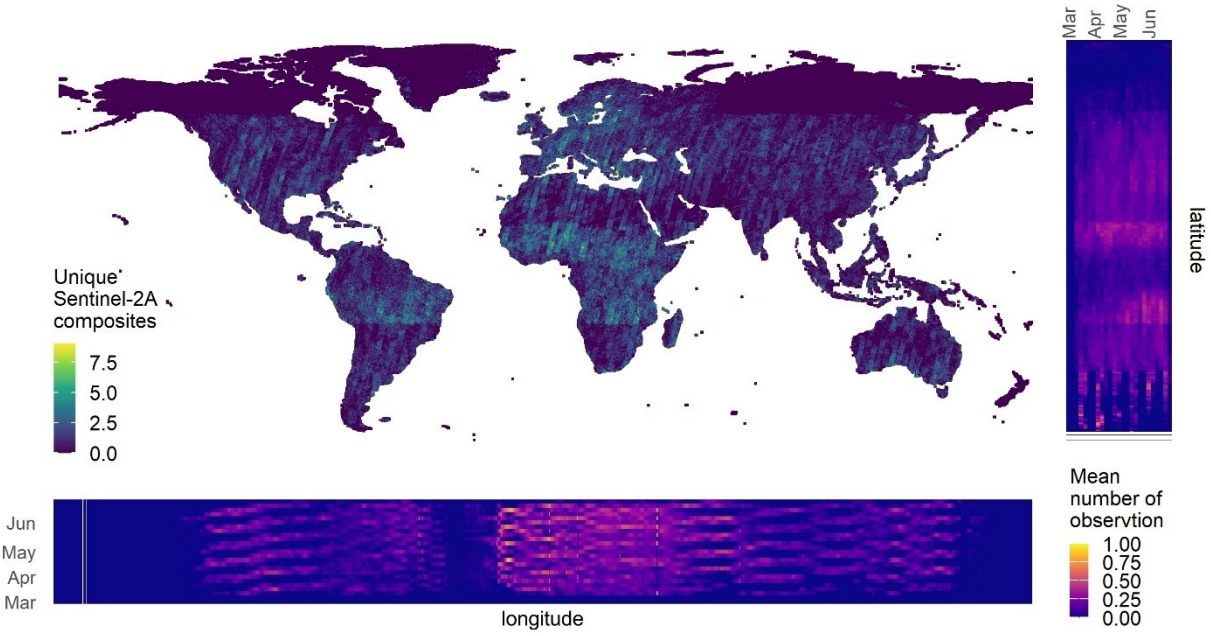

Figure S7 Tally of unique 5-day composites enabled by data from Sentinel-2A. Side panels show the latitude- and longitude-specific mean number of composites across time. Summary of all 5-day composites constructed based on all three Sentinel-2 platforms in Figure S8, and the proportional increase in Sentinel-2 5-day composites enabled by Sentinel-2A in Figure S9. Figure is in WGS 84 projection.

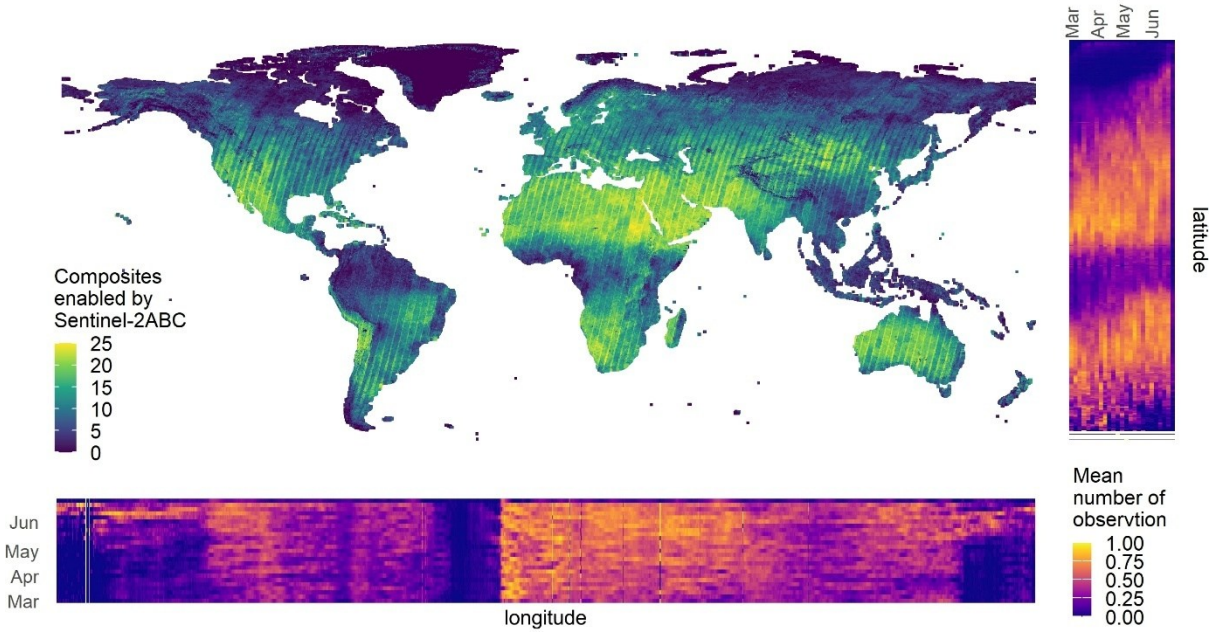

Figure S8 Tally of 5-day composites based on data from Sentinel-2A, -2B, and -2C. Side panels show the latitude- and longitude-specific mean number of composites enabled by the analyzed combination of platforms across time. Figure is in WGS 84 projection.

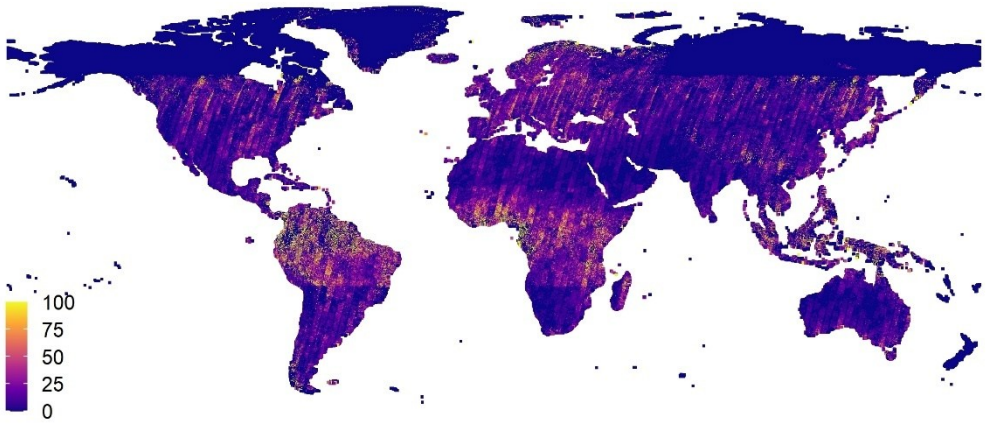

Figure S9 Proportional increase (%) in the number of 5-day composites ensured by cloud- snow-, and shade-free pixel-level Sentinel-2A acquisitions from March through June 2025, as compared to 5-day composites derived using the Sentinel-2B, and -2C baseline data pool. Figure is in WGS 84 projection.

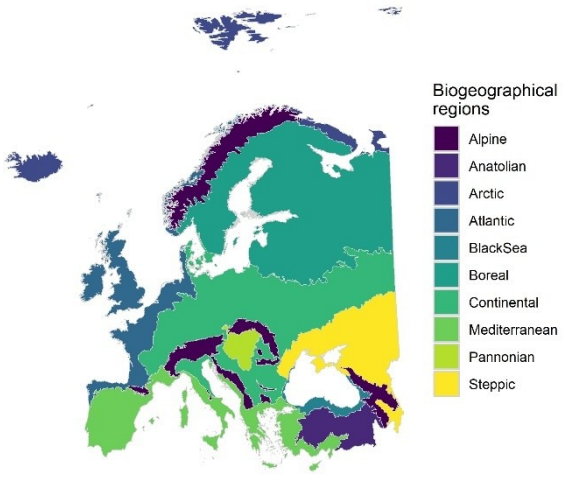

Figure S10 Biogeographical regions of Europe (Roekaerts, 2002). The spatial extent used in this analysis excludes Atlantic islands and extends eastwards to 66.9° N, 47.26° E - 46.04° N, 49.14° E. Figure is in WGS 84 projection.

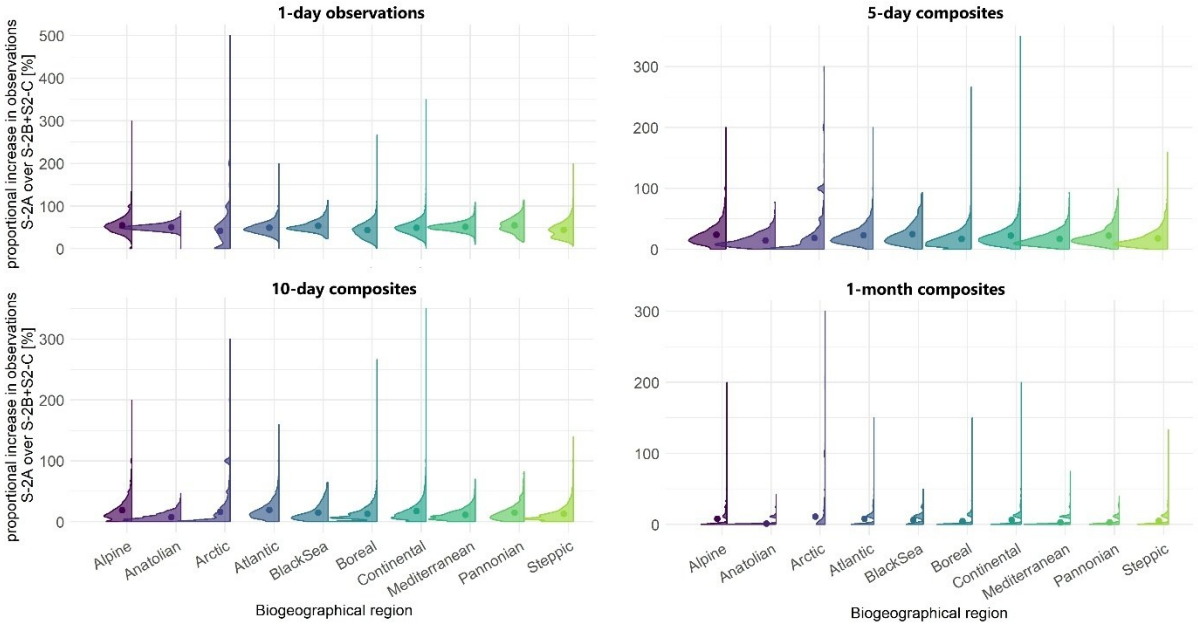

Figure S11 Violin plots showing the distribution of proportional increase (in %) ensured by Sentinel-2A usable observations and multi-day composites as compared to the Sentinel-2B and -2C baseline across biogeographical regions in Europe. The mean value for each distribution is represented by a dot. The width of each plot illustrates the relative number of observations in each bin. When no usable acquisitions were made by the Sentinel-2B and -2C baseline, the number of acquisitions made by Sentinel-2A was multiplied by 100%, i.e., values >100% may indicate either a manifold increase in the number of observations, or that there was no useful acquisition made by Sentinel-2B and -2C. Definition of adopted boundaries of biogeographical regions according to Figure S10.

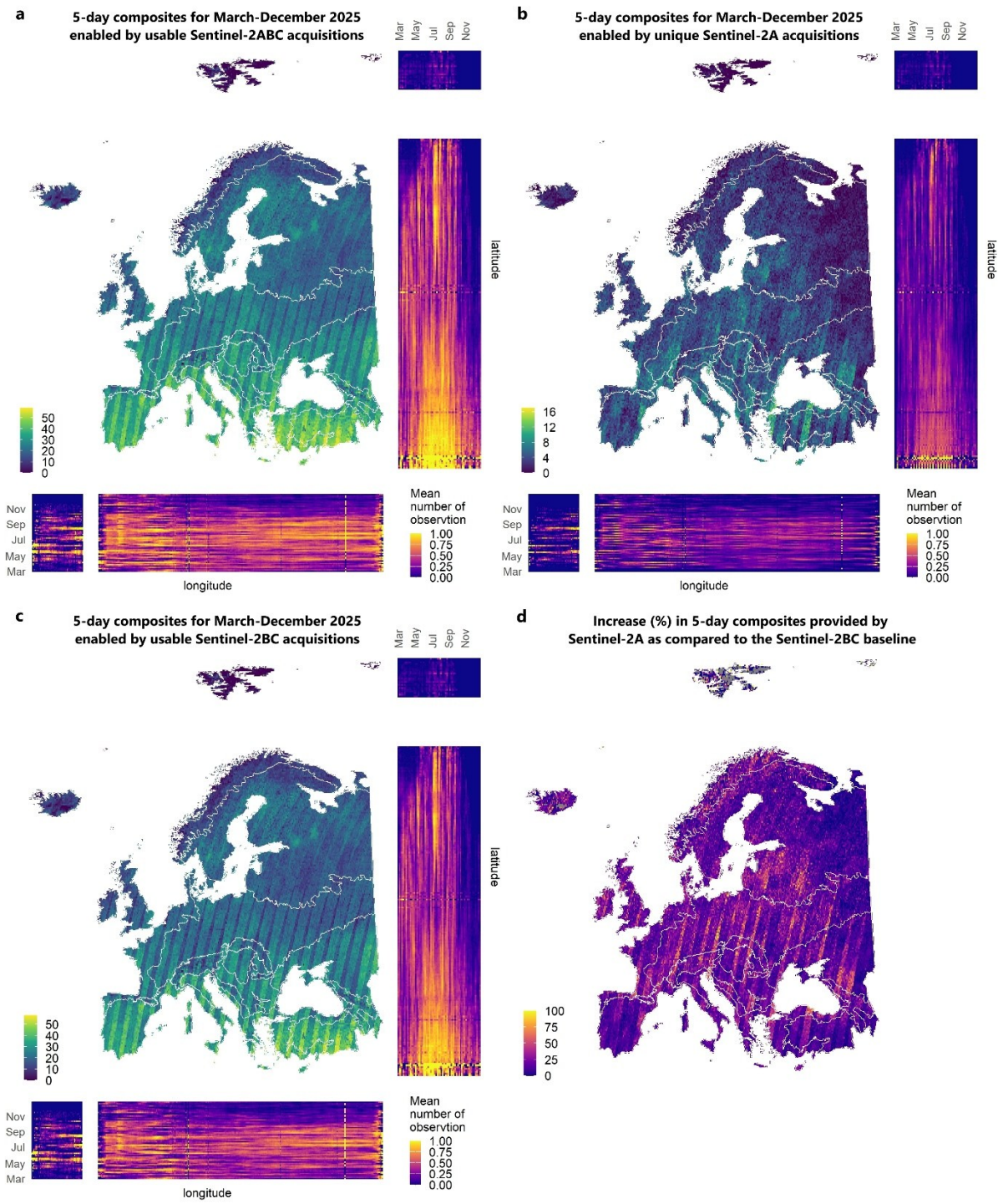

Figure S12 Comparison of the number of feasible 5-day composites enabled by usable observations acquired from March through December 2025 by (a) Sentinel-2A, -2B, and -2C, and (c) Sentinel-2B and -2C. In (b) unique 5-day composites for the same period enabled by Sentinel-2A acquisitions and in (d) the proportional increase (in %) of successful 5-day composites enabled by Sentinel-2A, as compared with the Sentinel-2B and -2C baseline. Side panels show the latitude- and longitude-specific mean number of usable acquisitions made by the corresponding combination of platforms. All panels plotted in WGS 84 projection.

References

Esri, Global Mapping International (GMI), n.d. World Continents [WWW Document]. URL https://hub.arcgis.com/datasets/esri::world-continents/ (accessed 2.9.26).

Roekaerts, M., 2002. The Biogeographical Regions Map of Europe Basic principles of its creation and overview of its development.